Int. J. Electrochem. Sci., 4 **(2009)** 1407 - 1418

International Journal of ELECTROCHEMICAL SCIENCE
www.electrochemsci.org

Application of DFT Method for Determination of IR Frequencies and Electrochemical Properties of 1,4-dihydroxy-9,10- anthraquinone-2-sulphonate

Siavash Riahi [1,2,*], *Solmaz Eynollahi*[2], *Shima Soleimani*[2], *Mohammad Reza Ganjali*[2,3], *Parviz Norouzi*[2,3], *Hamid Mohammad Shiri*[4]

[1] Institute of Petroleum Engineering, Faculty of Engineering, University of Tehran, P. O. Box 14399-57131, Tehran, Iran
[2] Center of Excellence in Electrochemistry, Faculty of Chemistry, University of Tehran
[3] Endocrinology & Metabolism Research Center, Medical Sciences/University of Tehran, Tehran, Iran
[4] Department of Chemistry, Tarbiat Modares University, P. O. Box 14115-175, Tehran, Iran
[*]E-mail: riahisv@khayam.ut.ac.ir

Received: 29 August 2009 / *Accepted:* 15 October 2009 / *Published:* 11 November 2009

Electrode potential of 1,4-dihydroxy-9,10- anthraquinone-2-sulphonate (quinizarin; QZ) was calculated in water**.** The calculated value was compared with the experimental value obtained by linear sweep voltammetry. DFT calculations with the 6-31G basis set have been used to compute the redox potentials for QZ. The resulting data illustrated that the method was likely to be useful for the prediction of biomolecules electrode potentials in different aprotic solvents. The dipole moment, electron affinity, ionization potential, electronegativity, absolute hardness, highest occupied molecular orbital (HOMO) and the energy of the lowest unoccupied molecular orbital (LUMO) were calculated in water. The IR frequencies and those intensities were calculated by DFT method.

Keywords: Redox reaction, 1,4-dihydroxy-9,10- anthraquinone-2-sulphonate, DFT, Solvent effect, Computational chemistry, IR spectrum, Chemometrics

1. INTRODUCTION

Dihydroxyquinones are compounds of significant chemical and biochemical interest. These molecules have important applications as a prominent family of pharmaceutically active and biologically relevant chromophores, as an analytical tool for the determination of metals, and in many aspects of electrochemistry. Quinizarin (1,4-dihydroxyanthraquinone is the simplest molecules showing the chromophore framework peculiar to several compounds of biological and pharmaceutical

interest. The former is present in some antitumor drugs as aclacinomycin, emodin, and hypericin and the latter in doxorubicin, daunorubicin, and adriamycin [1-4].

The main activities of these compounds arise from their reversible electron transfer behaviour [5-7]. The electro-oxidation of the compound in this category is well documented and involves a transfer of two electrons and two protons to provide the associated quinones [8-9]. The electron transfer process constitutes the basic feature of chemical, biochemical and, especially, electrochemical reactions. Therefore, the ability to calculate redox potentials accurately using the theoretical methods would be advantageous in a number of different areas, particularly where the experimental measurements are difficult, due to the complex chemical equilibria and the reactions of the involved chemical species. Recently, a number of reports, dealing with the electrode potential calculation of several biomolecules, have been published in the literature [10-13]. Computational studies have been widely used in drug [14-17], anticancer derivatives [18], and toxic compounds [19-30].

In this paper, the vibrational frequencies for QZ and QZH_2 were calculated using density function theory (DFT). Furthermore, standard electrode potential of half reaction, $E_{1/2}$, the electron affinity of the reduced species in the gas phase (EA), or the ionization potential for the reverse reaction (IP), the energy of the highest occupied molecular orbital (HOMO) or the energy of the lowest unoccupied molecular orbital (LUMO) and dipole moment of QZ and QZH_2 was also calculated at the same level.

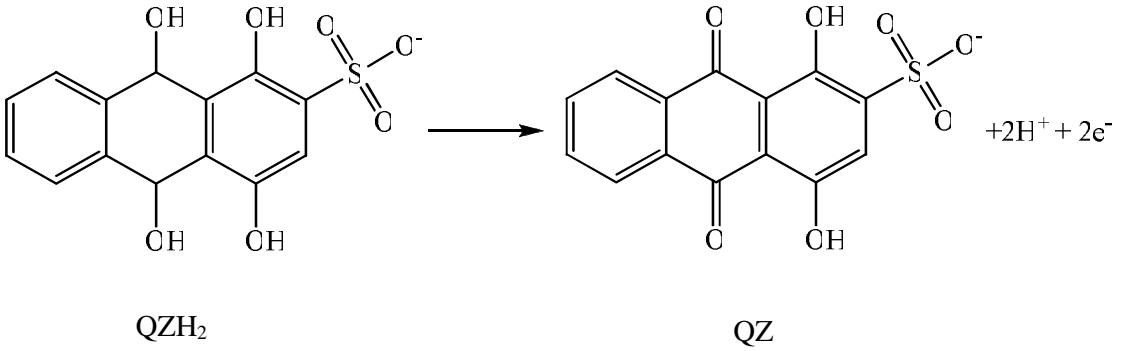

QZH_2 QZ

Scheme 1. Electron oxidation reaction which is for QZ

2. EXPERIMENTAL PART

2.1. Calculations

Scheme 1 depicts the two-electron oxidation reaction of the (QZ). The oxidized form (QZ) can also be converted to its reduced form (QZH_2) using catechol CAH_2 as a reference molecule, according to the following isodesmic reaction [31]:

$$QZ_{(sol)} + CAH_{2\,(sol)} \longrightarrow QZH_{2\,(sol)} + CA_{(sol)} \qquad (1)$$

The difference between the electrode potential of the two species can be obtained from the change in the Gibbs free energy of reaction (1), in accordance with the equation (2):

$$E^{o\prime} = E^{o'}_{CA} - \frac{\Delta G^{\circ}}{2F} \qquad (2)$$

Where ΔG° is the free energy change for reaction (1), $E^{o\prime}_{CA}$ is the experimental formal electrode potential for a reference molecule, $E^{o\prime}$ is the calculated electrode potential and F is the Faraday constant. The Gibbs free energy change for reaction (1) can be computed by the thermodynamic cycle depicted in Figure 1, which is used in the case of transferring all the involved species in the reaction from the gas phase into the solution phase [32].

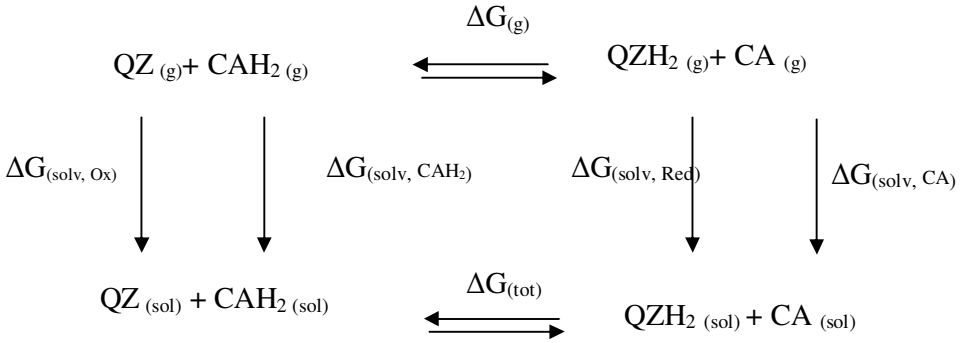

Figure 1. The thermodynamic cycle, proposed to convert the standard Gibbs energy of the isodesmic redox reaction in the gas phase to the standard Gibbs energy of the reaction in solution.

In order to calculate the standard Gibbs energy of reaction (1), ΔG°, one should calculate the standard Gibbs energy of each component, ΔG_i°, in reaction (1):

$$\Delta G^{\circ} = \sum \nu_i \Delta G_i^{\circ} \qquad (3)$$

where ΔG_i° the standard Gibbs energy of each component and ν_i is the stoichiometric coefficient. The standard Gibbs energy of each component is obtained using the following expression:

$$\Delta G_i^{o} = \Delta G_{i,gas}^{o} + \Delta G_{i,solv}^{o} \qquad (4)$$

where $\Delta G_{i,gas}^{o}$ is the gas-phase energy of each component and $\Delta G_{i,solv}^{o}$ is the solvation energy of the component. In the present work, the gas-phase contribution to the Gibbs energy, $\Delta G_{i,gas}^{o}$, was determined from ab initio calculation. These calculations have been performed at the HF and B3LYP using the 6-31G basis set [33-35]. The zero-point energies and thermal corrections together with entropies have been used to convert the internal energies to the Gibbs energies at 298.15 K. Solvation energies, $\Delta G_{i,solv}^{o}$, have been calculated using Polarisable Continuum Model (PCM) [36].

2.2 Softwares and equipments

The formal potentials (E°′) were reported in reference 37 [37]. A Pentium IV personal computer (CPU at 3.06 GHz) with the Windows XP operating system was used. The initial geometry optimization was performed with HyperChem (Version 7.0 Hypercube, Inc., Alberta, Canada). For all the ab initio calculation, Gaussian 98 has been employed [38].

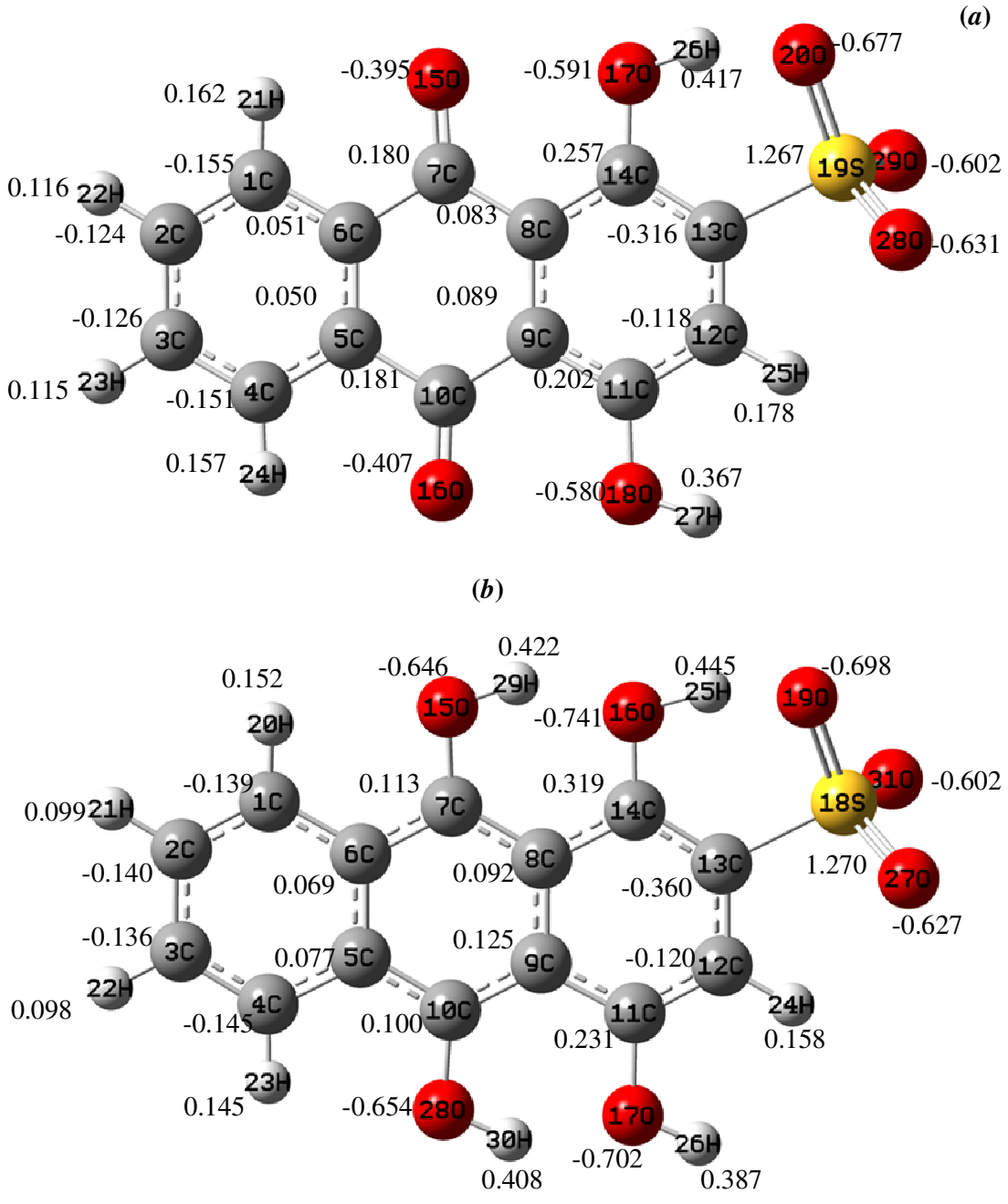

Figure 2. Optimized structures and atomic charges of (*a*) QZ and (*b*) QZH_2 in water by DFT method.

Table 1. The structural characteristics of QZ and QZH_2 in gas and solvent

	QZ		QZH_2	
	Gas	Solvent	Gas	Solvent
Bond length (Å)			Bond length (Å)	
R(1,2)	1.394	1.3938	R(1,2)	1.377	1.378
R(1,6)	1.405	1.4052	R(1,6)	1.426	1.428
R(1,21)	1.084	1.0837	R(1,20)	1.083	1.085
R(2,3)	1.405	1.4049	R(2,3)	1.425	1.424
R(2,22)	1.086	1.0857	R(2,21)	1.086	1.088
R(3,4)	1.393	1.3946	R(3,4)	1.377	1.379
R(3,23)	1.086	1.0859	R(3,22)	1.087	1.088
R(4,5)	1.405	1.4035	R(4,5)	1.428	1.428
R(4,24)	1.084	1.0839	R(4,23)	1.083	1.085
R(5,6)	1.402	1.4072	R(5,6)	1.438	1.437
R(5,10)	1.487	1.4944	R(5,10)	1.413	1.417
R(6,7)	1.493	1.4752	R(6,7)	1.415	1.416
R(7,8)	1.478	1.4531	R(7,8)	1.410	1.410
R(7,15)	1.255	1.2805	R(7,15)	1.377	1.382
R(8,9)	1.442	1.4429	R(8,9)	1.453	1.456
R(8,14)	1.423	1.4241	R(8,14)	1.446	1.444
R(9,10)	1.481	1.4724	R(9,10)	1.408	1.407
R(9,11)	1.410	1.4032	R(9,11)	1.438	1.444
R(10,16)	1.256	1.2568	R(10,28)	1.392	1.386
R(11,12)	1.403	1.4117	R(11,12)	1.366	1.367
R(11,18)	1.388	1.3829	R(11,17)	1.420	1.397
R(12,13)	1.371	1.3697	R(12,13)	1.414	1.420
R(12,25)	1.088	1.0913	R(12,24)	1.086	1.088
R(13,14)	1.416	1.4106	R(13,14)	1.379	1.378
R(13,19)	1.891	1.9175	R(13,18)	1.868	1.852
R(14,17)	1.349	1.3508	R(14,16)	1.372	1.381
R(17,26)	1.039	1.0046	R(15,29)	1.003	0.995
R(18,27)	0.979	0.9789	R(16,25)	1.108	1.034
R(19,20)	1.685	1.6444	R(16,29)	1.626	1.664
R(19,28)	1.644	1.6596	R(17,26)	0.974	0.997
R(19,29)	1.642	1.6445	R(17,30)	1.713	1.685
			R(18,19)	1.707	1.687
			R(18,27)	1.642	1.645
			R(18,31)	1.641	1.648
			R(28,30)	0.986	0.992
Bond angle (°)			Bond angle (°)		
A(2,1,6)	120.258	120.0809	A(2,1,6)	120.735	
A(2,1,21)	121.881	121.7341	A(2,1,20)	121.516	
A(6,1,21)	117.862	118.185	A(6,1,20)	117.748	
A(1,2,3)	120.041	119.9718	A(1,2,3)	120.240	
A(1,2,22)	119.953	119.9731	A(1,2,21)	120.134	
A(3,2,22)	120.006	120.0551	A(3,2,21)	119.626	
A(2,3,4)	119.937	120.1278	A(2,3,4)	120.505	
A(2,3,23)	120.056	119.9663	A(2,3,22)	119.528	
A(4,3,23)	120.007	119.9059	A(4,3,22)	119.967	
A(3,4,5)	120.189	120.3086	A(3,4,5)	120.723	
A(3,4,24)	121.836	121.8189	A(3,4,23)	121.358	
A(5,4,24)	117.976	117.8725	A(5,4,23)	117.919	
A(4,5,6)	119.902	119.4828	A(4,5,6)	118.714	

A(4,5,10)	119.121	118.9898	A(4,5,10)	121.524
A(6,5,10)	120.977	121.5274	A(6,5,10)	119.763
A(1,6,5)	119.674	120.0281	A(1,6,5)	119.083
A(1,6,7)	118.928	119.7544	A(1,6,7)	121.323
A(5,6,7)	121.397	120.2174	A(5,6,7)	119.594
A(6,7,8)	118.239	119.3099	A(6,7,8)	120.791
A(6,7,15)	117.909	118.7324	A(6,7,15)	117.069
A(8,7,15)	123.851	121.9577	A(8,7,15)	122.140
A(7,8,9)	120.263	120.9852	A(7,8,9)	119.570
A(7,8,14)	119.729	118.3691	A(7,8,14)	121.191
A(9,8,14)	120.005	120.6457	A(9,8,14)	119.240
A(8,9,10)	120.825	120.1669	A(8,9,10)	119.273
A(8,9,11)	119.105	117.7971	A(8,9,11)	117.106
A(10,9,11)	120.067	122.036	A(10,9,11)	123.618
A(5,10,9)	118.261	117.7932	A(5,10,9)	121.009
A(5,10,16)	118.558	118.5017	A(5,10,28)	116.157
A(9,10,16)	123.181	123.7051	A(9,10,28)	122.834
A(9,11,12)	120.183	120.5156	A(9,11,12)	122.582
A(9,11,18)	121.028	120.732	A(9,11,17)	116.324
A(12,11,18)	118.789	118.7524	A(12,11,17)	121.093
A(11,12,13)	120.464	121.7044	A(11,12,13)	119.612
A(11,12,25)	121.265	122.5218	A(11,12,24)	121.939
A(13,12,25)	118.257	115.7738	A(13,12,24)	118.409
A(12,13,14)	122.305	120.2934	A(12,13,14)	121.791
A(12,13,19)	116.267	115.359	A(12,13,18)	117.139
A(14,13,19)	121.322	124.3477	A(14,13,18)	120.990
A(8,14,13)	117.89	119.0438	A(8,14,13)	119.661
A(8,14,17)	121.703	122.3227	A(8,14,16)	118.170
A(13,14,17)	120.395	118.6335	A(13,14,16)	122.158
A(14,17,26)	109.614	109.1266	A(7,15,29)	108.260
A(11,18,27)	109.443	109.561	A(14,16,25)	107.774
A(13,19,20)	100.059	104.8161	A(11,17,26)	111.497
A(13,19,28)	103.792	99.666	A(13,18,19)	99.832
A(13,19,29)	107.097	104.8218	A(13,18,27)	105.378
A(20,19,28)	115.49	114.1998	A(13,18,31)	109.007
A(20,19,29)	113.345	116.5642	A(19,18,27)	114.237
A(28,19,29)	114.97	114.1929	A(19,18,31)	112.118
			A(10,28,30)	109.472

3. RESULTS AND DISCUSSION

F methThe geometrical optimization was the most significant step for the calculation of the formal electrode potential, on the grounds that the molecular parameters were controlled by the molecular geometry. The bond lengths and bond angles of the studied compounds were optimized by DFT and Hods (Figures 2a , 2b and Tables 1).

The most negative charge belongs to electronegative atoms oxygen and the most positive charge is sulfur atom because of was connected to three electronegative atoms.

For both the reduced and oxidized forms in the gas and solution phases, the calculated Gibbs energies of the molecules are summarized in Table 2, using DFT/6-31G. For the selection of 6-31G

basis set, the decisive factor was the size of the studied molecules. The computation of the solvation energies is considered an essential step, since these energy values are required for the conversion of the gas-phase energies to the energies in the solution phase. As a matter of fact, these solute–solvent interactions, calculated by the PCM solvation model [36], were added to the gas phase energies to give the Gibbs energy change of each component in the solution phase. Table 2 also lists the total Gibbs free energy of each component in the presence of water.

The thermochemistry values were calculated and were shown in Table 3.

Table 2. The Gibbs free energy of the studied molecules for both reduced (red.) and oxidized (ox.) forms in the gas phase and the solution phase, along with the change of the Gibbs free energy of reaction (1), ΔG_i^{o}, in both gas and solution phases [a]

	Mol.	$\Delta G^{o}_{i,gas}$ [b]		$\Delta G^{o}_{i,solv}$ [b]		ΔG_i^{o}	
		Red.	Ox.	Red.	Ox.	Gas	Solution
DFT/ 6-31G	QZ	-1463.084905	-1461.876428	-1463.167933	-1461.999171	-0.028687	0.022538
	CA	-380.95453	-379.77474	-380.98108	-379.78978	0	0

[a] Solution result was obtained with the PCM model
[b] These energies are in atomic units, Hartree (1 Hartree = 2625.49975 kJ mol^{-1})

Table 3. Calculated thermochemistry values

	QZ	QZH_2
Zero-point correction	0.193301	0.214145
Thermal correction to Energy	0.209089	0.231240
Thermal correction to Enthalpy	0.210033	0.232184
Thermal correction to Gibbs Free Energy	0.150002	0.169444
Sum of electronic and zero-point Energies	-1311.953649	-1313.123002
Sum of electronic and thermal Energies	-1311.937861	-1313.105907
Sum of electronic and thermal Enthalpies	-1311.936917	-1313.104963
Sum of electronic and thermal Free Energies	-1311.996948	-1313.167703

The attainment of CAQ electrode potentials was achieved with the aid of the total Gibbs energies and the experimental value of the electrode potential of the reference molecule, catechol (CA), in water (Eq. (2)) 10-13[8-11]. Table 4 presents the electrode potentials of the molecules, studied in water at the DFT/6-31G level. According to this Table, the electrode potentials of the molecules at this method and those obtained through experiments were found to be in a satisfactory agreement.

Table 4. Electrode potentials of the studied molecules, compared with the experimental values[a]. The differences (in mV) between the experimental and the calculated values are presented

Mol.[b]	Exp.(E°´(mV)) [c]	E°´ (mV)[d] (DFT/6-31G)
QZ	485	459
CAH_2	375	375

[a] Calculated by Equation 2 ($E^{o\prime} = E^{o'}_{CA} - \frac{\Delta G^{\circ}}{2F}$)

[b] Studied Molecules

[c] Experimental values.

[d] Electrode potentials calculated by Eq. (2) as explained in the text

Table 5 summarizes the highest occupied molecular orbital (HOMO), the lowest unoccupied molecular orbital (LUMO) and HOMO and LUMO energy gaps for $CAQH_2$ calculated at DFT level in the 6-31G basis set. The eigenvalues of LUMO and HOMO and their energy gap reflect the chemical activity of the molecule. LUMO as an electron acceptor represents the ability to obtain an electron, while HOMO as an electron donor represents the ability to donate an electron. The smaller the LUMO and HOMO energy gaps, the easier it is for the HOMO electrons to be excited; the higher the HOMO energies, the easier it is for HOMO to donate electrons; the lower the LUMO energies, the easier it is for LUMO to accept electrons. From the resulting data shown in table 5, it is obvious that the LUMO energies of $CAQH_2$ are lower than those of CAH_2 and the energy gap of $CAQH_2$ is smaller than that of CAH_2. Consequently, the electrons transfer from HOMO to LUMO in $CAQH_2$ is relatively easier than that in CAH_2. With the decrease of the LUMO energies, LUMO in $CAQH_2$ accepts electrons easily. The same methods were employed to study $CAQH_2$, also leading to the above stated conclusions and confirming the obtained results. Furthermore, dipole moment was calculated in the solvent and is shown in Table 5.

Table 5. The calculated amounts of HOMO and LUMO energies, dipole moment (μ), ionization potential (I), electron affinity (A), absolute electronegativity (χ) and absolute hardness (η) with the DFT/6-31G basis set

	QZ	QZH_2
E_{HOMO} (eV)	-3.30(-6.20) *	-2.02(-4.77)
E_{LUMO} (eV)	-0.34(-3.03)	1.12(-1.58)
E_{LUMO}- E_{HOMO} (eV)	2.96(3.17)	3.14(3.19)
μ	13.66(18.18)	12.04(18.19)
I	3.30(6.20)	2.02(4.77)
A	0.34(3.03)	-1.12(1.58)
χ	1.82(4.61)	0.45(3.18)
η	1.48(1.59)	1.57(1.59)

* The calculated parameters in water are presented in parenthesis

The calculated IR spectra of reduced and oxidizes forms were shown in Figures 3a and 3b, respectively.

Two important properties of any molecule (M) are its gas-phase ionization potential (I) and its electron affinity (A).

$$M(g) \rightleftarrows M^{+}(g) + e^{-} \quad I \qquad (5)$$

$$M(g) + e^{-} \rightleftarrows M^{-}(g) \quad A \qquad (6)$$

The determination of I and A allows the absolute electronegativity (χ) and absolute hardness (η) parameters for M to be calculated.

These quantities are defined as:

$$\chi = \frac{I + A}{2} \qquad (7)$$

$$\eta = \frac{I - A}{2} \qquad (8)$$

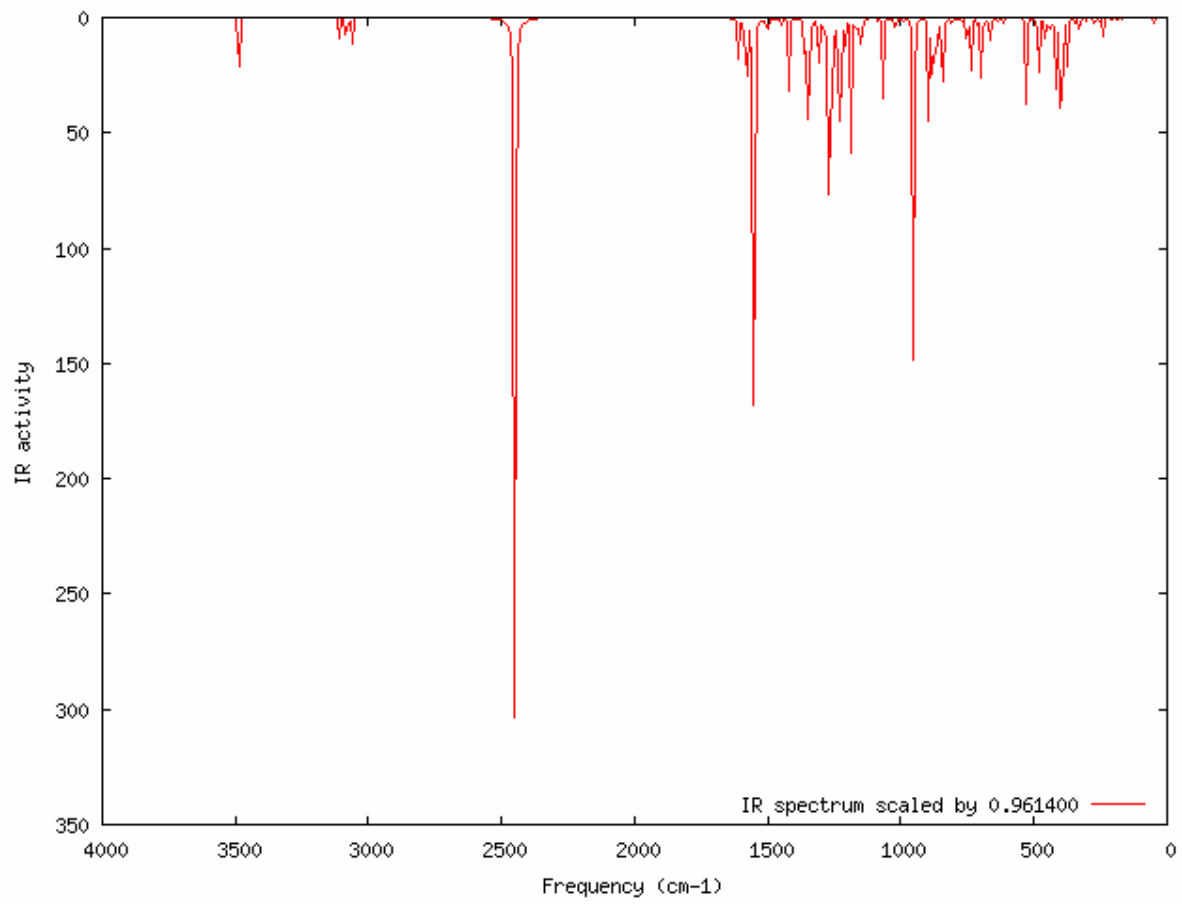

(a)

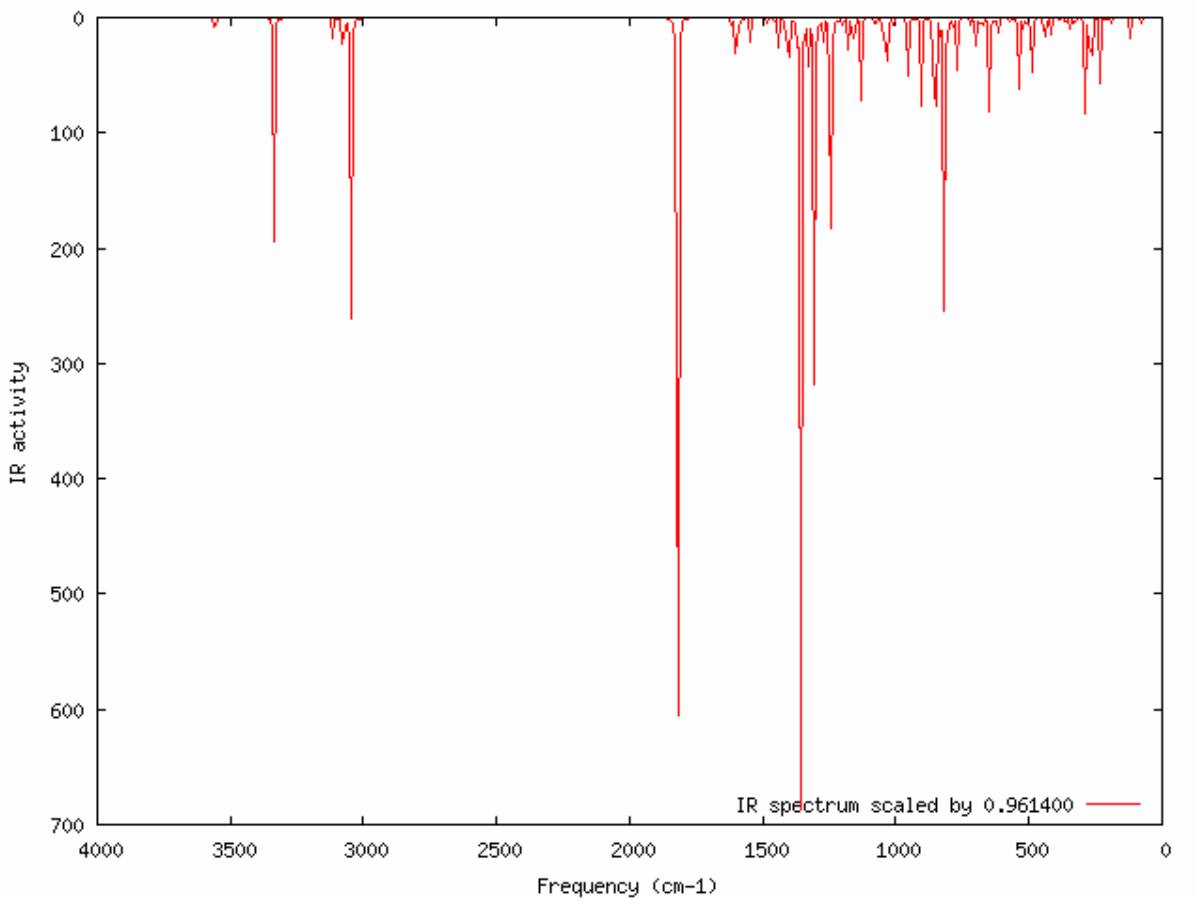

(b)

Figure 3. The calculated IR spectrum for (*a*) QZ and (*b*) QZH_2

In the most common case, I and A are related to the one-electron orbital energies of the HOMO and LUMO, respectively.

$$-I = E_{HOMO} \quad \text{and} \quad -A = E_{LUMO}$$

Then (I−A) is simply the difference in energy between the HOMO and the LUMO. Soft molecules have a small energy gap. Low 'I' creates a better electron donor and large 'A' makes a better electron acceptor.

4. CONCLUSIONS

For QZH_2 the formal electrode potentials were predicted with the help of DFT with the 6-31G basis set. It was revealed that the data from the experiments coincided with the predicted formal

electrode potentials for the QZH_2 half reactions. This theoretical method is very effective for the prediction of an unknown formal electrode potential of any compound involved in biochemistry. Since water make strong hydrogen bonding, it affects bonds contain oxygen atom.

In this paper we have showed some of the bond lengths, bond angles, dipole moment, electron affinity, ionization potential, electronegativity, absolute hardness, highest occupied molecular orbital (HOMO) and the energy of the lowest unoccupied molecular orbital (LUMO) have changed in water.

ACKNOWLEDGEMENT
We gratefully acknowledge generous allocations of computing from the Institute of Petroleum Engineering, University of Tehran for Advanced Computing and Supercomputing Facilities.

References

1. F. Arcamone, Doxorubicin: Anticancer Antibiotics, Academic Press, New York, 1981.
2. W.A. Remers, The Chemistry of Antitumor Antibiotics, Wiley, New York, 1981.
3. Y. Nonaka, M. Tsuboi, K. Nakamoto, *J. Raman Spectrosc.* 21 (1990) 133.
4. D. Jancura, S. Sanchez-Cortes, E. Kocisova, A. Tinti, P. Miskovsky, A. Bertoluzza, *Biospectroscopy* 1 (1995) 265.
5. O. S. Ksenzhek and S. A. Petrova, In "Electrochemical Properties of Reversible Biological Redox Systems", Nauka, Moscow (1986).
6. S. A. Petrova, M. V. Kolodyazhny and O. S. Ksenz-hek, *Electtoanal. Chem.,* 277 (1990) 189.
7. G. Dyrust, K. M. Kadish, F. Sehelier and R. Renneberg, *In "Biological Electrochemistry"*, Academic Press, New York (1982), p. 1.
8. H. H. W. Thijssen, *Pestic. Sci*., 43 (1995) 73.
9. S. Riahi, M. R. Ganjali, A. B. Moghaddam, P. Norouzi, G. R. Karimipour and H. Sharghi, *Chem. Phys*., 337 (2007) 33
10. Riahi, M. R. Ganjali, A. B. Moghaddam and P. Norouzi, *J. Theor. Comput. Chem. (JTCC),* 6 (2007) 331.
11. S. Riahi, M. R. Ganjali, A. B. Moghaddam and P. Norouzi, *J. Theor. Comput. Chem. (JTCC)*, 6 (2007) 255.
12. S. Riahi, M. R. Ganjali, A. B. Moghaddam and P. Norouzi, *Spectrochim. Acta, Part A*, 71 (2008) 1390.
13. S. Riahi, A. B. Moghaddam, M. R. Ganjali and P. Norouzi, *Int. J. Electrochem. Sci*., 4 (2009) 122.
14. M. R. Ganjali, P. Norouzi, F. S. Mirnaghi, S. Riahi and F. Faridbod, *IEEE Sens. J*., 7 (2007) 1138.
15. S. Riahi, M. R. Ganjali, A. B. Moghaddam and P. Norouzi, *Spectrochim. Acta, Part A*, 70 (2008) 94.
16. S. Riahi, M. R. Ganjali, P. Norouzi and F. Jafari, *Sens. Actuators, B*, 132 (2008) 13.
17. F. Faridbod, M. R. Ganjali, B. Larijani, P. Norouzi, S. Riahi and F. Sadat Mirnaghi, *Sensors*, 7 (2007) 3119.
18. S. Riahi, M. R. Ganjali and P. Norouzi, *J. Theor. Comput. Chem. (JTCC)*, 7 (2008) 317.
19. F. Faridbod, M. R. Ganjali, R. Dinarvand, P. Norouzi and S. Riahi, *Sensors*, 8 (2008) 1645.
20. S. Riahi, M. R. Ganjali, M. Hariri, S. Abdolahzadeh, P. Norouzi, *Spectrochim. Acta, Part A*, 74 (2009) 253.
21. S. Riahi, E. Pourbasheer, M. R. Ganjali and P. Norouzi, *J. Hazard. Mater.*, 166 (2009) 853.
22. M. F. Mousavi, M. Shamsipur, S. Riahi and M. S. Rahmanifar, *Anal. Sci*., 18 (2002) 137.
23. S. Riahi, M. F. Mousavi, M. Shamsipur and H. Sharghi, *Electroanal*., 15 (2003) 1561.

24. A. Moosavi-Movahedi, S. Safarian, G. H. Hakimelahi, G. Ataei, D. Ajloo, S. Panjehpour, S. Riahi, M. F. Mousavi, S. Mardanyan, N. Soltani, A. Khalafi-Nezhad, H. Sharghi, H. Moghadamnia and A. A. Saboury, *Nucleos. Nucleot. Nucl*., 23 (2004) 613.
25. H. Karami, M. F. Mousavi, M. Shamsipur and S. Riahi, *J. Power Sources*, 154 (2006) 298.
26. M. R. Ganjali, P. Norouzi, F. Faridbod, S. Riahi, J. Ravanshad, J. Tashkhourian, M. Salavati-Niasari and M. Javaheri, IEEE Sens. J., 7 (2007) 544.
27. M. R. Ganjali, T. Razavi, R. Dinarvand, S. Riahi and P. Norouzi, *Int. J. Electrochem. Sci*., 3 (2008) 1543.
28. M. R. Ganjali, M. Tavakoli, F. Faridbod, S. Riahi, P. Norouzi and M. Salavati-Niassari, *Int. J. Electrochem. Sci*., 3 (2008) 1559.
29. M. R. Ganjali, M. Hariri, S. Riahi, P. Norouzi and M. Javaheri, *Int. J. Electrochem. Sci*., 4 (2009) 295.
30. S. Riahi, F. Faridbod and M. R. Ganjali, *Sensor Lett*. 7 (2009) 42.
31. M. W. Wong, K. B. Wiberg and M. J. Frisch, *J. Am. Chem. Soc*., 114 (1992) 1645.
32. S. Riahi, A. B. Moghaddam, P. Norouzi, M. R. Ganjali, *J. Mol. Struct. (Theochem)*, 814 (2007) 131.
33. R. J. Driebergen, J. J. M. Holthuis, J. S. Blauw, S. J. Postma. Kelder., W. Verboom, D. N. Reinhoud and W. E. Van der Linden, *Anal. Chim. Acta*, 234 (1990) 285.
34. J. B. Foresman and A. E. Frisch, Gaussian Inc, Pittsburgh, PA (1998).
35. D. C. Young, Computational Chemistry, A Practical Guide for Applying Techniques to Real-World Problems, John Wiley & Sons, Inc., New York (2000).
36. C. J. Cramer, Essentials of Computational Chemistry: Theories and Models, 2nd ed, Wiley, Chichester (2004).
37. P. S. Guin, S. Das, P. C. Mandal, *Int. J. Electrochem. Sci.,* 3 (2008)1016.
38. M. J. Frisch, G. W. Trucks, H. B. Schlegel, G. E. Scuseria, M. A. Robb, J. R. Cheeseman, V. G. Zakrzewski, J. A. Montgomery, R. E. Stratmann, J. C. Burant, S. Dapprich, J. M. Millam, A. D. Daniels, K. N. Kudin, M. C. Strain, O. Farkas, J. Tomasi, V. Barone, M. Cossi, R. Cammi, B. Mennucci, C. Pomelli, C. Adamo, S. Clifford, J. Ochterski, G. A. Petersson, P. Y. Ayala, Q. Cui, K. Morokuma, D. K. Malick, A. D. Rabuck, K. Raghavachari, J. B. Foresman, J. Cioslowski, J. V. Ortiz, B. B. Stefanov, G. Liu, A. Liashenko, P. Piskorz, I. Komaromi, R. Gomperts, R. L. Martin, D. J. Fox, T. Keith, M. A. Al-Laham, C. Y. Peng, A. Nanayakkara, C. Gonzalez, M. Challacombe, P. M. W. Gill, B. Johnson, W. Chen, M. W. Wong, J. L. Andres, C. Gonzalez, M. Head-Gordon, E. S. Replogle, and J. A. Pople, Gaussian, Inc., Pittsburgh PA (1998).